IOP Conf. Series: Journal of Physics: Conf. Series **825** (2017) 012018 doi:10.1088/1742-6596/825/1/012018

Anode energy transfer in a transient arc

F Valensi[1*], P Ratovoson[1], M Razafinimanana[1] and A Gleizes[1,2]
[1] *LAPLACE (Laboratoire Plasma et Conversion d'Energie), CNRS-INPT-Université Toulouse III, 118 Route de Narbonne, 31062 Toulouse cedex 9, France*
[2]*CNRS, LAPLACE, 118 route de Narbonne, 31062 Toulouse Cedex 9*

E-mail : flavien.valensi@laplace.univ-tlse.fr

Abstract. This work deals with experimental investigation of a transient arc. Arc configuration and electrode erosion were studied in order to quantify the energy transfer to the electrodes as a function of maximal current, time constant and electrodes material. Experiments with two consecutive arcs allow demonstrating non stationary behaviour of the arc electrode interaction. This is due to the fact that while the duration of the experiments is far larger than plasma phenomena time constants, it is comparable to those of electrode heating and melting processes.

1. Introduction

Transient arc can occur during the separation of contacts in an electric circuit. They are characterized by a short duration of a few milliseconds to a few hundreds of milliseconds. The current can reach high value, usually at least a few hundred or a few thousand amperes. Such arcs occur in circuit breakers operation [1] but can also be observed in rail transportation systems when the contact is lost between the pantograph and the overhead line [2]. In this case the arc can lead to significant degradation of the electrode material (particularly the contact strip of the pantograph) in addition to abrasive wear. The distance between the electrodes can increase from near contact to a few millimeters or even a few centimeters. This means that the voltage drop of the arc is at least a few tens of volts and the resulting power is high enough to cause strong electrode erosion. Both electrodes are degraded but the damages are more important at the anode. It is then important to get a better understanding of the involved phenomena in order to further improve the systems performances. In particular a lot of efforts are made to increase the lifetime of the electrodes contacts by developing new materials. The work reported here is dedicated to the study of electrode erosion for graphite and copper contacts. Samples made of pure materials have been tested as well as a two components electrodes made of graphite loaded with 25% Cu. The general arc behavior is first presented for several arc conditions (current maximal value, duration of the pulse and electrode gap). Then the anode erosion is studied for the three materials and the results are discussed in term of energy.

2. Experimental setup

The arc is generated using a capacitor bank discharge. The maximal current and the time constant of the RC circuit can be set independently; detailed description of the setup is given in [3]. The arc discharge is triggered by the closure of a thyristor: the current rises up to its maximal value in less than one millisecond, according to the thyristor switching on characteristic. Indeed, the VSKT162/12PBB modules used for this setup can reach their nominal continuous current (160 A) in a few microseconds according to the datasheet but the current rise slope decreases for high current in pulsed mode operation. The arc initiation can be performed with a small copper wire (for small electrode gap) or without contact between the electrodes by applying a high voltage pulse when the thyristor closing is triggered. The current then decreases following quite closely the exponential decay of a RC circuit.

The arc phase ends when the voltage becomes too low but it is also possible to shut down the arc after a given delay with a time step of 1 ms. However due to the thyristor technology the switching off is not instantaneous and arc actual extinction occurs a few milliseconds later. The capacitor bank can also be split in two independent parts, thus allowing double shots separated by a few milliseconds. Experiments were performed with peak current up to 2 kA and time constants from 24 to 92 ms. In the case of double arcs the delay was set to 12 ms.
The cathode is made of a 6 mm cylindrical graphite rod with tapered end. Two anode diameters (6 mm and 15 mm) were used in the case of copper; tests with graphite were performed with a 10 mm diameter anode. The square contact strip samples (25 wt.% Cu) were 15 mm wide. In all experiments the anode thickness was about 10 mm. The height of the cathode tip above the anode (h) can be set from 1 to 10 mm. The arc geometric configuration and electrode erosion are observed with high speed camera (Phantom V9) using acquisition speed from 4000 to 6000 fps. Two filters were used, one centred at 515 nm (FWHM: 20 nm), corresponding to Cu I emission lines and one centred at 750 nm (FWHM: 25 nm), corresponding to N I emission lines. This allows to get qualitative information about plasma composition and the repartition of elements coming from the anode (copper) or already present in the gas (nitrogen). The mass loss is measured by weighting the samples before and after each experiment. In addition the electrode ablation can be monitored during the arc through high speed imaging and the surface of the anode samples are observed after arc extinction. The electrical parameters (arc current I and voltage U) were also recorded with a time resolution of 25 μs.

3. Results and discussion

3.1. Arc shape and electrode erosion observation

The typical shape of the arc corresponds to a cone with the tip at the cathode for all studied anode materials. An example is shown in figure 1 for a 6 mm diameter copper anode with three values of maximal current and a time constant of 24 ms. This behavior can be attributed to Maecker effect, as a result of the electromagnetic force producing a pinch at the cathode tip [4]. Then the arc behaves more like a constricted arc than a free burning arc, which is consistent with results found in literature for short length (< 1 cm) and high current (> 100 A) arcs [5]. The comparison of images obtained with interference filters centered on copper and nitrogen lines provides qualitative information on these elements repartition. While nitrogen is distributed rather homogeneously in the plasma, a darker zone (indicating a low neutral nitrogen concentration area) can always be observed below the cathode for imaged recorded with the filter centered on nitrogen lines [3]. This can be explained by the prevalence of ionized lines over neutral lines considering the high temperature (> 20 000 K) [5,6] encountered. Its size differs according to the nature of the anode material: it is larger and can be observed for a longer time with pure graphite than with copper containing anode. This effect can be attributed to the higher plasma cooling due to strong copper vapor concentration and consequently increased radiation losses.

a) b) c)

Figure 1. Arc shape (λ = 515 nm) 0.5 ms after ignition; 6 mm copper anode, h= 4mm, τ = 24 ms: a) I_{max} = 500 A, b) I_{max} = 1000 A and c) I_{max} = 2000 A.

Some information about electrode erosion can be obtained from the high speed image recording. In the case of pure graphite anodes the mass loss is limited and the erosion seems to be a continuous process. This is consistent with the fact that carbon directly sublimates and there is no molten phase. When the

anode is constituted by a mixture of carbon and copper the erosion is slightly higher, but the main difference is that one can observe small particles ejected from the surface of the anode. In contrast the erosion of pure copper anodes is much stronger and large deformation of the electrode can be observed. Metal droplets are ejected from the arc attachment area and in the case of 6 mm diameter anodes, melted copper can flow down from the surface.
While the current decreases along the discharge following an exponential decay, the maximal erosion is not observed at the beginning of the arc. In the first step, the presence of copper vapor is weak and no electrode deformation is visible. Then the erosion increases and the arc radiation is dominated by metallic lines while the melting of the anode surface becomes visible. Finally, at the end of the arc, radiation from nitrogen is dominant again and no more anode erosion occurs. The time needed to reach significant erosion and the duration of the highest erosion step as a function of operating parameters is reported in table 1.

Table 1. Duration of the steps associated to 6 mm diameter copper anode erosion (h = 4 mm).

Maximal current I_{max} (A)	Time constant τ (ms)	Erosion beginning (ms)	Maximal erosion (ms)
500	24	3	6-8
	41	3	8-12
	91	3	40-70
1000	24	2	8-16
	41	2	8-20
2000	24	1.25	8-16

It appears that the first step depends mainly on the maximal current but the time constant of the discharge has no influence on its duration. On the other hand, the time needed to reach maximal erosion depends on both parameters. However at high current (1000 and 2000 A) there is no more effect of current increase which can be attributed to minimal time needed to heat up and melt the electrode. When a 15 mm diameter anode is used, the deformation of the electrode is reduced (no molten metal flowing from the electrode) and the erosion is less irregular. The duration of the first step remains unchanged (for instance, 2 ms for a 1000 A current) but the time needed to reach maximal erosion is shorter (between 6 and 10 ms). The duration of the observable erosion step is also reduced, which can be explained by the fact that the heat flux is transferred on a larger volume in the case of larger anode samples. The power needed to heat and melt the electrode is greater and the time during which erosion is possible is reduced.

3.2. Anode ablation measurement

3.2.1. Ablated mass. We have shown in a previous work [3] that the mass loss increases with current and time constant is more than ten times higher with copper than with graphite for a 6 mm diameter anode. It is negligible in the case of graphite for a current of 500 A and reaches 4.8 mg ± 5% for τ = 24 ms and I_{max} = 2000 A. Under the same conditions it is up to 150 mg ± 9% for copper. These results are consistent with the fact that graphite appears to be ablated only through sublimation (at 4100 K) while copper melts at 1357 K. While copper vaporization also occurs, melted metal can also leave the anode as ejected droplets which significantly increases mass loss in the case of small diameters anodes.

3.2.2. Parametric study. The first studied parameter is the anode diameter. In the case of graphite (where the results are not influenced by electrode melting) the results for a 1000 A arc are given in table 2. The last column shows the total electrical energy for the test. It appears that the ablation decreases when diameter increases as reported by Heberlein et al. [7]. For short length arcs and flat anodes, arc attachment is quite diffuse as one can see in figure 1. However the anodic root expansion is limited due to magnetic pinch effect and thermal and electrical conductivity effects in the solid

metal. For low current, the anodic root dimension is smaller than the anode diameter and very low ablation occurs, especially with refractory material such as graphite. Energy loss through conduction and convection are dominant and few energy is available for electrode erosion. The latter then increases with current. When it is high enough so that the anodic root reaches the size of the anode, further increase will lead to higher current density, especially on the edge of the electrode. The power transferred to the anode and the resulting ablation will then significantly increase with current.

Table 2. Ablated mass for I_{max}=1000A (τ= 41ms), h = 4 mm.

Material	ϕ (mm)	Ablated mass (mg)	Uncertainty (%)	Energy (J)
Graphite	6	2.46	5.03	1223
Graphite	10	1.08	4	1158
Copper	6	53	10.6	1091
Copper	15	6.3	8.9	998

This explains why for a given current the anode ablation is weaker when the diameter is larger. Besides, the material volume which must be heated before erosion occurs is larger. In the case of graphite, our experimental conditions correspond to the low erosion mode, below the current limit yielding to higher erosion. On the opposite, there is a strong difference between the two tested diameters in the case of copper. Results tend to show that the anodic root is smaller than 15 mm and in this case the ablation remains weak.

The second studied parameter is the arc duration. It depends on the time constant but the possibility to cause arc extinction at a chosen time also allows studying the evolution of erosion over time. The results for copper anodes with diameter of 6 and 15 mm and an arc length of 2 mm are shown in figure 2. It appears that erosion increases over time during about 50 ms before it reaches a plateau (figure 2a). This confirms the fact that below a given value of current the erosion becomes negligible: at this time the intensity of the current becomes lower than 300 A. The behavior is similar for the 15 mm diameter electrode (figure 2b) but the increasing erosion step is much shorter. Strong erosion occurs only during the first 5 ms.

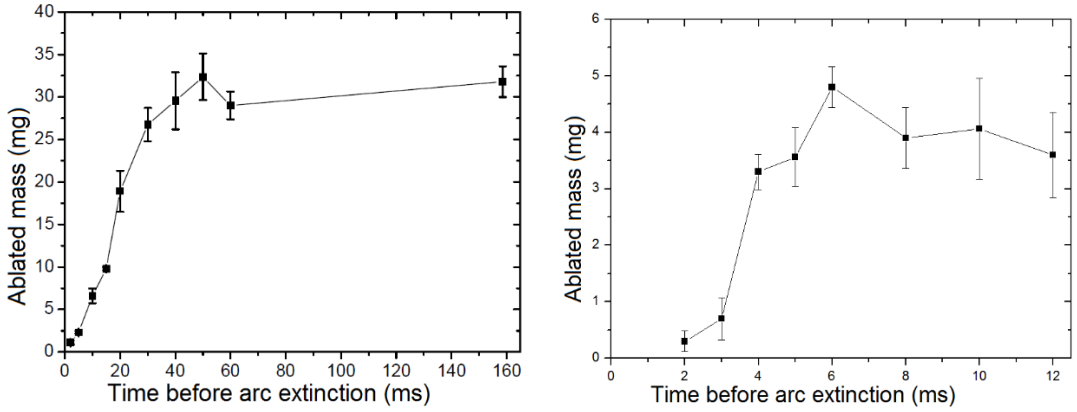

a) b)

Figure 2. Ablated mass as a function of arc duration for h = 2 mm, I_{max}=1000A; a) anode diameter of 6 mm and τ= 41 ms, b) anode diameter of 15 mm, and τ= 27 ms

The high erosion step duration appears to be different when the arc length changes from 4 to 2 mm. In order to further investigate, this evolution of ablated mass has been studied as a function of the arc length. The peak currents set at 1000 A and a time constant of 41 ms for copper anodes. The results for the two tested anode diameters (6 and 15 mm) are presented in figure 3. In the case of the smaller diameter the influence of arc lengths seems to be low but results show clearly an increase of mass loss from 2 to 4 mm. While for the larger anode diameter, the ablation is lower the behavior is the opposite. There is a strong decrease in ablation when arc length increases, even if for distance greater than 8 mm

there is also the beginning of a plateau. Then for a given arc root extension, the size of the anode seems to have determinant influence on the dependence of arc length.

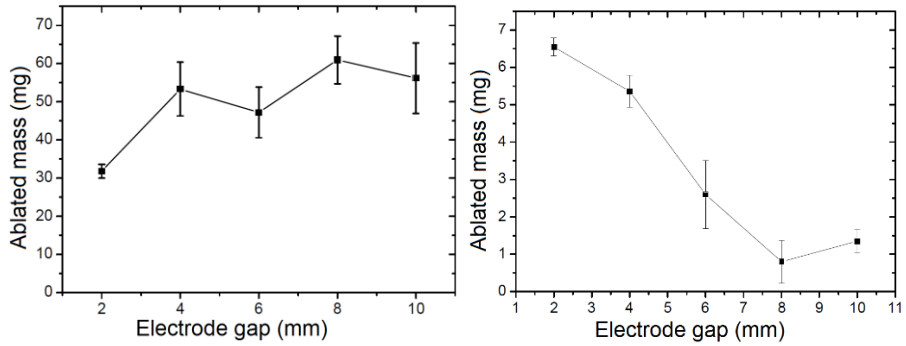

a) b)

Figure 3. Ablated mass as a function of electrode gap h for I_{max}=1000A and τ= 41ms; a) copper anode diameter of 6 mm, b) copper anode diameter of 15 mm

3.2.3. Comparison with literature. In the case of copper anode, our work can be compared to those of Devautour *et al*. [8] with arc duration between 5 and 20 ms, current ranging from 200 and 1000 A and electrode diameter of 8 mm. The ablated mass at anode increases from 1 to 2 mg for maximal current of 400 and 600 A, respectively and reaches 6 mg at 1000 A. These results are comparable to ours for the 6 mm diameter anode for the two lowest values and for the 15 mm anode for the highest. This corresponds to conditions where arc attachment is smaller than the electrode diameter. The influence of arc length in the case of carbon anodes has been studied by Mentel *et al*. [9]: for electrode gap which does not exceed 1 cm, the electrode ablation increases as a function of arc length. The correlation between energy transfer and electrode erosion can be considered by relating ablation to current intensity (or electrical power) at a given instant or to the energy for a given period. When the current intensity is not constant over time the ablation can also be related to electric charge [10]. For a graphite anode, our results show that the ablation is negligible for current below 500 A. Then, one can consider the total electric charge Q_{tot} (integration over all the pulse duration) and the partial charge Q_{par} corresponding to the time during which current is greater than 500 A. We have reported the values we get using this method in table 3.

Table 3. Ablated mass and electric charge for the graphite anode.

I_{max} (A)	τ(ms)	ϕ(mm)	Q_{tot}(C)	Q_{par} (C)	m (mg)	m/Q_{tot} (mg/C)	m/ Q_{par} (mg/C)
2000	24	6	46,8	35,5	4,78	0,102	0,134
1000	24	6	20,6	10,84	1,23	0,06	0,114
	41	6	34,8	18	2,46	0,07	0,137
		10	34,8	18	1,08	0,031	0,06

When considering the calculation for the entire pulse, our results are in agreement with those of Lefort *et al.* [10] experimentally obtained with a current of 70 A (0.05 mg/C). The values they calculated for currents of 1000 A and more (0,16 mg/C) are also compatible with that we obtained with small diameter electrodes when considering only time during which current is above 500 A.

3.3. Energy transfer at the anode

3.3.1. Arc total power and energy. The instantaneous total power injected in the arc can be calculated from instantaneous current and arc voltage:

$$p(t) = u_{arc}(t) \times i(t) \quad (1)$$

with

$$u_{arc} = u_{col}(t) + u_{elec}(t) \quad (2)$$

In equation (2), $u_{col}(t)$ corresponds to the arc column voltage and $u_{elec}(t)$ the electrodes voltage drop. The power temporal evolution for three currents is shown in figure 4. It appears that the power is always smaller with copper, which can be attributed to smaller voltage drop and the strong presence of metal vapors leading to decrease the arc voltage with this material [11].

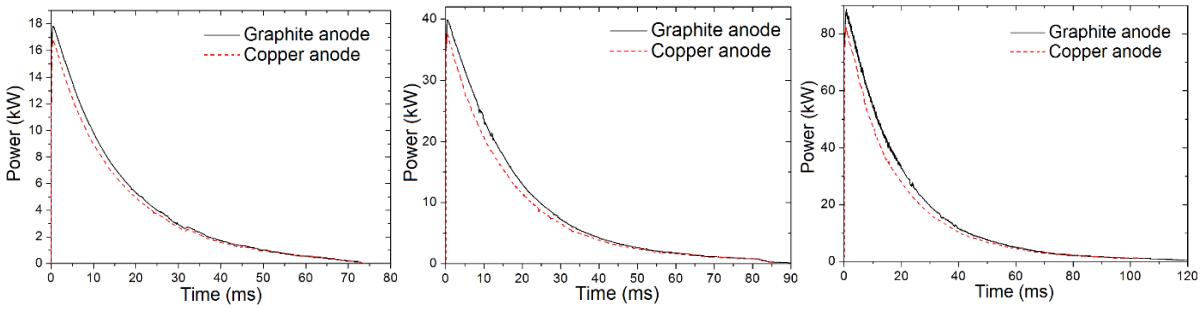

Figure 4. Total power injected in the arc for copper and graphite anodes, τ = 24 ms:
a) I_{max} = 500 A; b) I_{max} = 1000 A; c) I_{max} = 2000 A.

The total energy can be calculated by integrating instantaneous power over the total discharge time. Results are presented in table 4 for three currents, three time constants and both anode material. For each case, according to results above, the arc energy is greater with graphite than with copper.

Table 4. Total injected energy for graphite and copper anodes.

I_{max} (A)	Time constant τ (ms)	Total injected energy E (J)	
		Graphite	Copper
500	24	298	275
	41	522	479
	91	1238	1083
1000	24	731	651
	41	1223	1091
2000	24	1823	1595

3.3.2. Estimation of anode energy transfer. The energy transferred to the anode (for a 200 A arc [12]) corresponds mainly to about 70 % of the quantity $(V_a + \phi_s)\times j_e$, where V_a is the anode voltage fall, ϕ_s the material work function and j_e the current density. When integrating over the anode surface, it yields to $(V_a + \phi_s)\times I$. The work function for copper and graphite is 4.5 and 4.9 eV, respectively. Higher uncertainties are associated to anode voltage fall and various values can be found in literature ([5], [13]). On the basis of our previous results [11] the voltage can be estimated to a few volts (at least 1 V). Considering that the power transferred to the anode P_{anode} is proportional to current it can be written as:

$$P_{anode} = I.\ U_{anode} \quad (3)$$

With the equivalent voltage V_{anode} equals to 9.5 V ± 1.5 V. This represents 20% to 30 % of total voltage for arc length of 1 cm to a few mm. Then one can consider that the energy transferred to the anode can reach one third of arc total energy in our experimental conditions.

3.3.3. Correlation between energy transfer and ablation – arc length influence. In order to consider the influence of deposited energy on material ablation, the most relevant criterion is the power density. According to results presented in figure 3, two different anode diameters lead to different values and evolution as a function of arc length for ablated mass. When electrode gap increases, the voltage and the electric power increase. This leads to higher arc radiation loss that contributes to heat up the anode,

(even if in our conditions radiation is not the main contribution of the energy balance). For a longer arc, the anodic root size increases and the power density at the anode is lower which means less ablation. This occurs for arc shorter than a few cm, for greater length the anodic root is constricted. Two plasma jets from both electrodes join in a diffuse intermediary region [14]. Considering that the anode voltage fall remains constant when arc length increases, it is then possible to explain the contradictory behavior observed in figures 3a and 3b. For small anode diameter, the anodic root covers all anode surface and when arc length increases the ablation moderately increases due to higher radiation transfer from the arc. For greater anode diameter, the arc root (initially smaller than anode diameter) increases with arc length, which decreases the power density and then the ablated mass.

3.4. Copper anode vaporization

3.4.1. Procedure for estimation of the vaporized mass. The mass loss that is obtained from weighting measurements corresponds to melted (and ejected as droplets) and vaporized metal. The high speed imaging of the arc has shown that copper vapors are present during all the discharge, even if the amount is very low for the first milliseconds [3]. The mass of metal required to get visible copper vapor is very low (0.1 mg for a 100 ms arc) when compared to the measured ablated mass (1 to 150 mg).

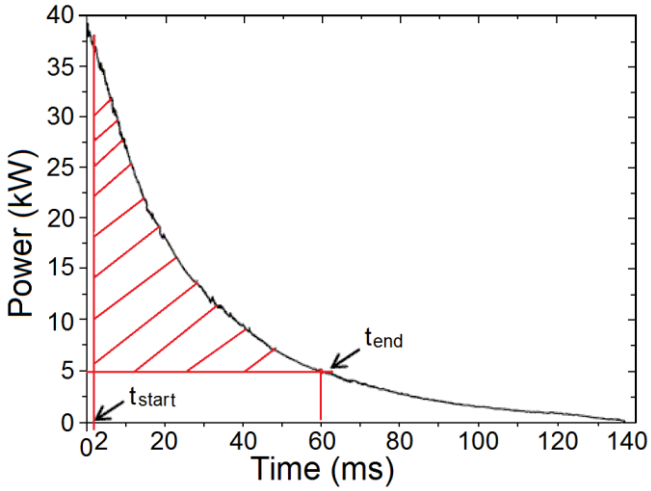

Figure 5. Arc power (I_{max} = 1000 A, τ = 41 ms, h = 4 mm): the hatched part indicates the arc energy that is available for anode ablation.

Then, qualitative detection of metal vapor in the arc is not sufficient to estimate the vaporized part. All energy transferred to the anode (representing up to one third of total power) is not directly responsible of mass loss, since the electrode must be heated up (at least up to copper melting temperature) before ablation occurs. In addition, the ablation ends before arc extinction as shown in figure 2. One can consider that ablation ends 60 ms after arc ignition of a 1000 A arc with a time constant of 41 ms (the plateau starts at 50 ms). The graphic representation of the arc energy available for ablation is presented in figure 5, the actual ablation energy representing one third of it.
The start and end of ablation are indicated as t_{start} and t_{end}. The corresponding minimal power needed for electrode erosion is 5 kW. These two instants cannot be evaluated with precision and while the relative uncertainty over t_{stard} has low consequences (t_{start} ranges from 1 to 3 ms) the appreciation of t_{end} is more critical. While the mass loss measurements as a function of time (figure 2) lead to a value of t_{end} between 40 and 60 ms, high speed observation tends to show anode erosion up to 80 ms. In order to get a parameter independent of time constant and arc duration, the current corresponding to time of ablation end has been considered. This intensity ranges from 200 and 400 A for the three studied currents and time constants. The energy responsible for anode ablation is then obtained by integrating the power according to these limits (hatched part of figure 5) and multiplying the result by 0.3. Results are presented in table 5.

Table 5. Estimation of the energy needed (in J) for copper anode ablation (6 mm diameter, h = 4 mm)

Energy (J)	I_{max}=500A			I_{max}=1000A		I_{max}=2000A
$I_{end\ of\ erosion}$ (A)	τ=24ms	τ=41ms	τ=91ms	τ=24ms	τ=41ms	τ=24ms
400A	2.13	4.78	10.59	53.46	89.34	241.02
316A	7.68	15.24	34.29	69.9	118.92	275.07
300A	9.27	16.83	37.8	73.35	124.05	283.86
200A	20.52	37.62	84.33	97.74	167.58	328.17

These values of energy have to be interpreted considering the energy needed to heat and melt solid copper then to heat and vaporize liquid copper. For a mass of 1 g it corresponds to 583 J (when starting at room temperature) and 5454 J, respectively.

3.4.2. Discussion. On the basis of high speed imaging, one can consider that for current below 500 A (where ablation is low) the anode surface presents a small melted pool with low perturbation and that copper ablation is mainly due to vaporization (no ejected droplets). Then, for a current of 500 A the energy available for anode erosion (presented in table 5) is roughly equal to the energy needed to vaporize the ablated mass (table 6). This corresponds to a current threshold between 316 and 363 A, which is in agreement with the results of ablation measurement as a function of time presented in figure 2. Then a value of 340 ± 24 A can be considered. The melted and vaporized part of copper can then be calculated from the thermophysical data indicated above, the energy available and the ablated mass. The results for the three currents and time constants are given in table 6.

Table 6. Estimation of the melted and vaporized quantities of copper for a 6 mm diameter anode.

I_{max} (A)	Time constant τ (ms)	Ablated mass (mg)	Energy needed for total ablated mass vaporization E_{vap} (J)	Estimated melted mass (mg)	Estimated vaporized mass (mg)
500	24	1.05	6.4	0	1.05
	41	1.72	10.5	0	1.72
	91	2.78	17	0	2.78
1000	24	14.81	90.7	10.1	4.71
	41	53.03	324.8	13.65	39.38
2000	24	150.6	922	29.2	121.4

For current below 500 A, the ablated mass corresponds mainly to vaporized matter. When current increases the contribution from metal that is melted and ejected (as droplets) from the anode is greater. For the highest intensities, the melted part becomes dominant when compared to vaporized part. These conclusions are valid for small diameter anodes, where the arc anode root covers the entire electrode surface event at low current.

3.5. Application to the carbon-copper electrode

In addition to pure graphite or copper electrodes, experiments were made with contact strop samples that contain 75 wt.% carbon and 25wt.% copper. At low current (500 A and τ = 91 ms) the mass loss (3 ± 0.6 mg) is similar to that observed with copper anodes. For higher current the ablation does not increase as much as for copper but is greater than for graphite. For instance with a maximal current of 1000 A (and a time constant of 41 ms) the mass losses are 2.5 ± 0.25 mg, 6.3± 0.57 mg and 4.1± 0.19 mg for graphite, copper and graphite-copper anode samples, respectively. Then there is no simple relation between the composition and the erosion resistance of the material.

As in the case of copper or graphite, the influence of ablated mass as a function of arc length (electrode gap) has been studied. The results for two currents and time constants (I_{max} = 500 A, τ = 91

ms and I_{max} = 1000 A, τ = 41 ms) are presented in figure 6. While the anode size is larger than the arc root the ablation increases with arc length, contrarily to copper with identical conditions. High speed imaging shows that in this case arc root size decreases for greater arc length, leading to higher power density and higher erosion. In addition, one has to consider that copper and graphite anodes are solid homogeneous materials while the graphite-copper samples are produced through sintering, resulting in non-homogeneous materials.

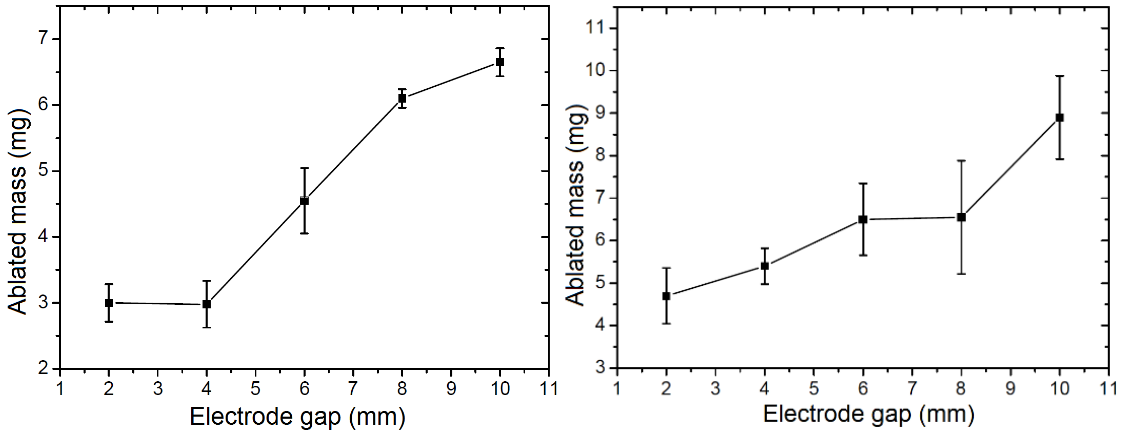

Figure 6. Ablated mass as a function of electrode gap h for C+25wt.% Cu anodes
a) I_{max}=500A and τ= 91ms; b) I_{max}=1000A and τ= 41ms;

The influence of the electrode temperature evolution has been studied through multiple successive arc experiments. The results have been obtained with one arc with extinction triggered after 6 ms and two 3 ms arcs separated by 9 ms delay. While the duration of the high current step is the same for both experiments, the ablation appears to be smaller in the second case: it drops from 4.8 ± 0.29 mg to 2.9 ± 0.21 mg in the case of pure copper. The trend is similar for the graphite-carbon mixture (from 1.4 ± 0.07 mg to 1.1 ± 0.08 mg) even if the difference is smaller. These results can be related to the heating process of the electrode. When the arc is extinguished after 3 ms the material starts cooling down and needs to be heated up again during the beginning of the second pulse. Then, even if the total time for high power is the same as for the 6 ms arc, less energy is available to cause material ablation. This proves that the anode temperature evolution is relevant considering the arc time scale: the time needed to heat up the electrode is not negligible when compared to the duration of the studied arcs. A duration of 9 ms is sufficient to lead to significant electrode cooling. This justifies that the non-stationary aspect of the plasma-electrode interaction has to be considered.

4. Conclusion

The results show that the ablation in the case of copper is much stronger than in the case of graphite. The influence of geometric (anode size and arc length) and electric (maximal current and pulse duration) parameters has been studied for both materials. For a given anode sample, there is a current intensity threshold (320 A for copper and 500 A for graphite) below which no significant erosion occurs. The size of the anodic root has been found to be determinant on ablation mechanism. The repartition between melted and vaporized metal leaving the anode is also dependent on current: at low intensity (500 A) vaporization is dominant while at higher current intensities (1000 and 2000 A) ejection of melted metal droplets becomes the main matter loss mechanism. The erosion for a mixture of graphite and copper is higher than with pure graphite, but lower than with pure copper. This composition (25 wt.% Cu) seems to correspond to a good compromise between electrical conductivity (higher for copper) and material ablation resistance (higher for graphite). Besides it is known that friction wear resistance is higher with large graphite content.

Acknowledgements: The authors wish to thank Pr. A. Mpanda from ESIEE (14 quai de la Somme, BP10100 - 80082 Amiens Cedex 2, France.) for the contact strip samples.

References

[1] McBride J W and Weaver P M 2001 Review of arcing phenomena in low voltage current limiting circuit breakers *IEE Proc.-Sci. Meas. Tech* **148**-1 pp 1–7

[2] Bormann D, Midya S and Thottappillil R 2007 DC components in pantograph arcing: Mechanisms and influence of various parameters *Proceedings of 18th International Zurich Symposium on Electromagnetic Compatibility, Munich, Germany* pp 369–372

[3] Ratovoson P, Valensi F, Razafinimanana M and Tmenova T 2014 Spectroscopic study and high speed imaging of a transient arc *Journal of Physics: Conference Series* **550** 012012

[4] Finkelnburg W and Maecker H 1956 Electric Arcs and Thermal Plasmas In: *Encyclopedia of Physics*, vol. XXII, Springer-Verlag, Berlin

[5] Hsu K C, Etemadi K and Pfender E 1983 Study of the free-burning high-intensity argon Arc. *J. Appl. Phys*. **54** pp 1293-1301

[6] Freton P, Gonzalez JJ, Camy F, Peyret and Gleizes A 2003 Complementary experimental and theoretical approaches to the determination of the plasma characteristics in a cutting plasma torch. *J. Phys. D : Appl. Phys.* **36**, pp 1269-1283

[7] Heberlein J, Mentel J and Pfender E 2010 The anode region of electric arcs: a survey. *J. Phys. D: Appl. Phys.* **43** 023001 (31p)

[8] Devautour J, Chabrerie J P and Testé Ph 1993 The study of thermal-Processes in an electrode submitted to an electric-arc *J. Physique III* **3** pp 1157-1166

[9] Mentel J and Heberlein J 2010 The anode region of low current arcs in high intensity discharge lamps. *J. Phys. D: Appl. Phys.* **43** 023002 (20p)

[10] Lefort A, Parizet MJ, El-Fassi SE and Abbaoui M 1993 Erosion of Graphite-electrodes *J. Phys. D: Appl. Phys.* **26** pp 1239-1243,

[11] Valensi F, Ratovoson L, Razafinimanana M, Masquère M, Freton P and Gleizes A 2016 Electrode voltage fall and total voltage of a transient arc, *J. Phys. D: Appl. Phys.* **49** 255202 (13p)

[12] Lago F 2004 In: *Modélisation de l'interaction entre un arc électrique et une surface: application au foudroiement d'un aéronef*, Ph.D Dissertation, Université Paul Sabatier, Toulouse III

[13] Lowke J J, Morrow R, Zhu P, Haidar J, Farmer A J D and Haddad G N 1992 The physics of free burning arc and their electrodes *Journal of High temperature chem. Processes* pp 549-556

[14] Bauchire J M, Hong D, Rabat H and Riquel G 2012 Radiation of transient high-current arcs: energy measurements in the optical range *Journal of Physics: Conference Series* **406** 012030